# Modelling Methodologies for Quality Assessment of 3D Inkjet Printed Electronic Products

S. Stoyanov*, G. Tourloukis, T. Tilford, C. Bailey

University of Greenwich, London, UK

* s.stoyanov@gre.ac.uk, +44 20 8331 8520

*Abstract*

*Achieving optimal performance, quality and reliability is a key factor for the success and adoption of 3D printing technology in electronics manufacturing applications. This paper presents modelling methodologies and toolsets that can help in addressing these 3D inkjet printing process challenges. The main discussions are on (1) Modelling the structural behaviour of typical printed electronics structures using finite element analysis and (2) Condition based monitoring (CBM) for product quality/performance using machine learning techniques. Advanced capabilities in finite element modelling and data-driven techniques are employed in order to enable the assessment of the material behaviour of the ink-based materials during printing and in their post-cure state. Demonstrations of the modelling capabilities with respect to both approaches are given with representative study cases. Results show that layer-by-layer build up can lead to structural weakness and dimensional inaccuracy in the third dimension due to cure shrinkage. Model predictions offer quantitative analysis of the cure shrinkage effects and can inform on optimal material selection and process conditions. Data from measurements and sensors can enable diagnostics and prognostics predictions and thus help achieving product specification requirements.*

## 1 Introduction

3D printing technologies offer the possibility to fabricate parts and products in a cost-effective, high-throughput, mass-customisation and energy efficient manner across a diverse range of applications [1]. One growing application of 3D printing includes the fabrication of electronic structures and components such as thin-film transistors, conductive and photovoltaic structures, mechanical actuators and sensors [2]. Recent advances in the technology suggest that 3D printing has the potential and can transform the traditional, based on assembly of components and partially integrated circuits, manufacture of electronic products into printing-based manufacture of completely integrated devices with functional capabilities [2,3].

ASTM Standard F2792 "Standard Terminology for Additive Manufacturing Technologies" generically defines seven process classifications for additive manufacturing, specifically Binder Jetting, Directed Energy Deposition, Material Extrusion, Material Jetting, Powder Bed Fusion, Sheet Lamination, and Vat Photopolymerization [4]. The approach to respective material deposition and the layer formation varies with the different additive manufacturing processes. For example, in the case of directed energy deposition focused thermal energy (i.e. energy source such as laser, electron beam, or plasma) is used to fuse materials by melting as they are being deposited. Inkjet printing method is an example of a material jetting method. It involves the ejection of continuous or drop-on demand ink droplets from a printhead nozzle and their deposition and solidification on a selected substrate. Figure 1 illustrates the operating principle of 3D inkjet printing process with a piezoelectric printhead.

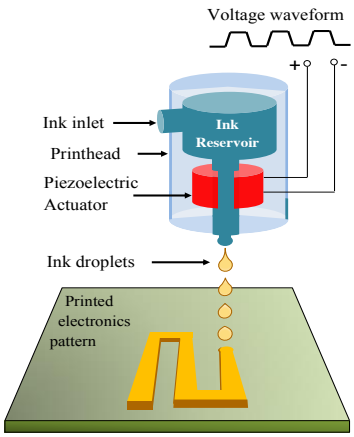


*Figure 1: Schematic outline of 3D inkjet printing process*

For the manufacture of nearly any electronic device by means of 3D printing to become reality, present challenges related to performance, quality and reliability of printed electronics have to be successfully addressed.

Dimensional and shape accuracy of printed structures and achieving required specifications (e.g. resistivity of conductive lines, etc.) is a major requirement. The quality of 3D inkjet printing process is highly dependent on both material physical properties and machine

ISBN 978-3-8396-1001-5

operating conditions such as the droplet ejection, deposition and cure [5]. Computational intelligence techniques such as artificial neural networks, fuzzy systems and genetic algorithms have been used for quality prediction in a variety of applications but so far have found limited use in relation to 3D printing processes. Work published to date is mainly in the field of rapid prototyping [6]. For example, the use of a combined back propagation neural network and genetic algorithm has been investigated for predicting values of critical 3D bio-printing process parameters [7].

From reliability point of view, risks of stress-induced defects in a final product are of great concern and have to be mitigated or, at least, understood. Majority of the research activities to date in this area have focussed on analysis of the structural stability of 3D printable designs. As an example, Stava et-al studied stress relief design solutions based on hollowing and thickening using finite element analysis [8]. Although stability issues are important for many printed products, these are not particularly relevant for printed electronics where stress-driven failure modes associated with delamination and crack formation are of prime interest.

This paper presents advanced modelling methodologies and toolsets that can enable optimal 3D inkjet printing process design through modelling the structural behaviour of printed products using finite element analysis and condition based monitoring for product quality using machine learning techniques. Focus is on predicting stress in 3D printed electronics due to cure shrinkage. The approach enables predicting in transient manner the stress build-up and the structural interactions between the printed layers as they are sequentially deposited and cured. Demonstrations of the modelling capabilities with respect to both approaches are given with representative study cases.

## 2 Thermo-mechanical modelling of 3D inkjet-printed structures

3D inkjet printing is based upon depositing in a layered manner materials which are initially in liquid state (inks) and then must be cured as part of the overall manufacturing process in order to achieve their final solid state. As a result of these processing steps, the properties of the printed materials change over time. A method of implementing a curing process simulation for ink-based materials in terms of predicting the final product shape and respective residual stress state due to shrinkage is investigated and demonstrated.

### 2.1 Modelling approach and analysis

Viscoelastic-related shrinkage is the dominant source of stress when 3D inkjet-printed structures are fabricated. This is a key factor affecting the quality of the products in terms of their dimensional and shape accuracy. Shrinkage behaviour of polymers is not always fully characterised and hence such material data or models are typically not available. Volumetric cure shrinkage for most unfilled polymers is typically around 3% to 5%. The availability of mechanical properties of the cured materials can enable achieving accurate model predictions for the behaviour of the materials during processing but also how they perform in their final cured state.

The chosen strategy to model the viscoelastic-related shrinkage and associated stresses that develop during the curing process of the printed layers is to deploy relevant finite element models. Cure shrinkage in either thermal cure process or UV cure can be simulated through the standard FEA codes capability for modelling the thermal expansion phenomenon. This requires the calculation of so called effective coefficient of thermal expansion ($\alpha_{eff}$). The strains caused by the temperature driven thermal expansion ($\varepsilon_T$) and the chemically-induced cure shrinkage ($\varepsilon_C$) are modelled respectively as:

$$\varepsilon_T(t) = \alpha(T(t) - T_0)\ , \text{ and } \quad \varepsilon_C(t) = bp_m(t) \qquad (1)$$

where $\alpha$ is the polymer coefficient of thermal expansion (CTE), $T(t)$ is temperature as function of time, $T_0$ is reference temperature, $b$ is total chemical strain at the end of cure (negative value for shrinkage) and $p_m$ is mechanical degree of cure. The mechanical degree of cure is a measure of the polymer mechanical integrity and is used as a representation of the degree of cure of the polymer. Given that the viscosity of the uncured material is very small, storage modulus for uncured polymer can be effectively taken as zero. Therefore, the mechanical degree of cure can be obtained as the ratio of the storage modulus at time $t$ during the cure polymerisation process and the maximum storage modulus achieved at the end of the cure.

The total strain ($\varepsilon_{tot}$ ) is a sum of the thermal strain and the chemical cure strain:

$$\varepsilon_{tot}(t) = \left(\alpha + \frac{bp_m(t)}{T(t)-T_0}\right)(T(t) - T_0) \qquad (2)$$

This equation allows a direct input into a FEA code for the effective coefficient of thermal expansion as function of time:

$$\alpha_{eff}(t) = \alpha + \frac{bp_m(t)}{T(t)-T_0} \qquad (3)$$

In the case of UV cure process where thermal effects are extremely short and localised, the simulation can assume no temperature change and hence no thermal strains. The sequence of layer(s) deposition of ink material and their cure is simulated with a finite element model through simulation restarts. At each restart, the mesh elements in the domain of the deposited layer(s) are activated as well as the mesh elements of the already cured layers beneath. Respective material properties are defined at each restart to account for the modulus of the

ISBN 978-3-8396-1001-5

previously cured layers as well as the change in modulus of the layer(s) cured at the current simulation step. The calculations for the cure strain, the mean by which cure shrinkage is modelled and predicted, is triggered at each simulation step (restart) using an artificial thermal load with respective reference temperature. CTE is set to zero so that no thermal strain exists. Using finite element capability for elements activation and deactivation (birth and death, as in ANSYS [11]), the domain of mesh layers yet to be printed (i.e. above the current layer ) are kept deactivated and are not solved until the printed structure is built to that thickness.

As with the thermal strains, cure shrinkage can cause stress in the solid printed structure. These stresses depend on the printed design, for example if the structure is printed on a substrate or on supporting structure made from same material. Also, multi-material structures will shrink by different amount based on their cure shrinkage properties and this can results in shrinkage-driven miss-match and stress. This is the typical case with printed electronics where conductive tracks are printed on top or imbedded into insulating polymer materials. Understanding stress levels caused by shrinkage can help identify rules, materials and design layouts so that stress is reduced, respectively improved product reliability is achieved.

The main data requirements for the outlined finite element modelling approach include topology and geometry of the printed layers, curing sequence, data on volumetric shrinkage of cured materials, and mechanical properties of cured materials. The thermo-mechanical analysis with this investigation is undertaken using ANSYS software [11].

### 2.2 Demonstration study

In a typical electronics application, 3D inkjet printing process is used to manufacture conductive tracks on or inside insulating material layouts. The problem investigated in this study case aimed at model-based characterisation of:

(1) Shrinkage phenomena and how it affects quality of printed structures in terms of deviation from target shape dimensions.

(2) Stress due to sequential layer cure shrinkage miss-match and bi-material layouts.

The baseline printed structure consists of 10 layers of insulating material. The thickness of a single layer deposited as liquid ink is 25 microns. As per Table 1, the model captures the effect of 3.0 % volumetric cure shrinkage of the insulating ink following UV cure. UV cure is assumed to take place after each layer is deposited. As a result, the deposition of the ink material per layer occurs always on top of already cured previous layers. A finite element model of the 10-layer domain is developed. The analysis is based on a sequence of 10 simulation restarts, each modelling the deposition/cure of a layer in the built-up structure, with appropriate definition of active and deactivated elements as well as respective material properties.

The materials used to print the structures are defined with the properties listed in Table 1.

*Table 1: Material properties of insulating and conductive inks in post-cure state*

| Materials | Volumetric shrinkage, % (post cure) | Elastic Modulus, GPa (post cure) |
|---|---|---|
| Conducting material, Ag-based ink | 2.0 | 7.0 |
| Insulating material | 3.0 | 2.0 |

A key model assumption made here is that the first layer is deposited on a rigid substrate. This affects the boundary condition specified with this model. In this case the bottom surface of the very first layer is restricted to displace in-plane and out-of-plane. It is also assumed that a new liquid layer is printed always as per the target in-plane layer dimension and thickness.

The predictions from this simulation are for deformation and stress. The displacement results are due to shrinkage and capture all inter-layer interactions; thus they inform about the final predicted shape and how it may deviate from the CAD-defined original target shape. Figure 2 illustrates the set of modelling results showing the state of the structure after printing each of the 10 layers. The contours refer to the von Mises stress and detail the stress pattern at the edge of the printed structure. The shape of the layers is the deformed shape illustrated with magnification factor 5. The red dotted lines define the original target topology of the 10 layers, with each layer thickness being 25 microns (total target thickness 250 microns). Finally, the grey layer is a schematic representation where the current 25 microns thick layer of liquid ink is deposited.

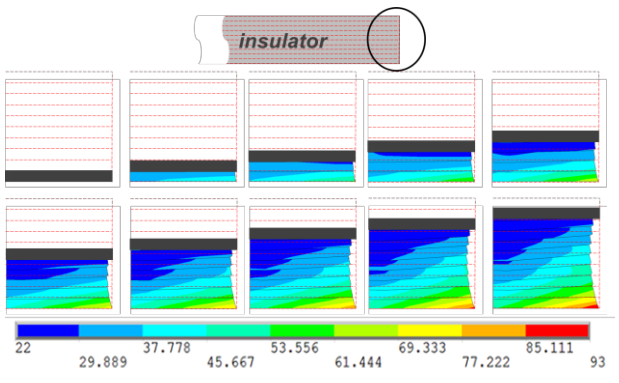


*Figure 2: Model predictions for deformation (shape due to cure shrinkage magnified by factor F=5) and contour levels of von Mises stress (MPa) in case of insulating material only 10-layer structure*

ISBN 978-3-8396-1001-5

Under the model assumption of printing directly on a solid material substrate, the following main conclusions from this analysis are derived:

1. Highest stress develops at the edge region of the first layer. This is driven predominantly by the fixation of the bottom layer to substrate.
2. Away from edge region, stress is very low. This is due to printing layers of same material that have matching cure shrinkage.
3. In terms of the cross sectional profile, at the periphery of the domain of printed layers, there is a lateral offset due to cure shrinkage. This in-plane shrinkage is limited as cured layers beneath provide significant restriction for deformations in this direction. The first few layers from bottom show gradual increase in in-plane shrinkage as the volumetric balance of new layer in relation to cured layers is not that large. With more layers deposited and cured, it becomes more difficult for a newly cured layer to deform laterally as its deformation is restricted by the solid layers beneath. Only local edge effects driven by shrinkage occur (as shown in Figure 2).
4. The volumetric shrinkage affects substantially the thickness of the printed structure because out-of-plane (vertical) direction is the one that allows natural free shrinkage of any new layer that is deposited. In this study case, the final structure has total thickness of 244 microns compared against target specification of 250 microns.

Demonstrated model predictions can be used to identify adjusted specification for the layer thickness so that the error due to shrinkage is compensated, and the final structure complies with target dimensions.

In the scenario of releasing the printed structure from the substrate, some of the stress built into the cured layers due to the fixture to the substrate will be relaxed. There will still be some residual stress remaining. These residual stresses are negligible across the layered structure if made by single material, as in the case of insulating material only. This is shown in Figure 3.

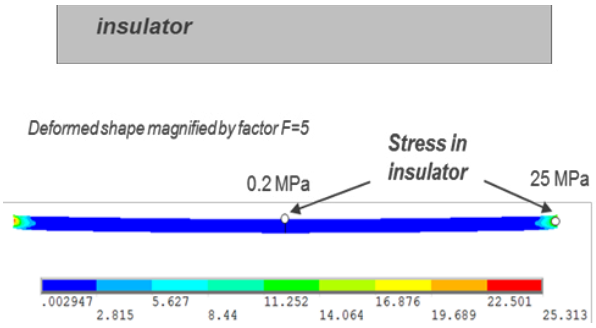


*Figure 3: Model prediction for von Mises stress and deformation of a 10-layer printed insulating material strture after release from substrate*

There is also no major deformation (bending) as no multi-material cure shrinkage miss-match is present. Stress at the peripheral edge of the structure is predicted with the model but these have also dropped substantially compared with the stress state when the printed structure was fixed to the substrate.

Figure 4 details the scenario for similar 10-layer printed structure, with the same layer topology and thickness as the insulating structure, but this time there is a 50 microns conductive material layer deposited with printed layers #7 and #8. In this case residual stress and deformation are affected by the difference in the cure shrinkage between the insulating and conducting materials. Stresses are higher as a result of the stiffer conductive layer and this introduces the risk of delamination failure. The model predicted that the insulating material layers printed on top of the conductive layer are subjected to higher stress compared with those beneath. It should be noted that if interfacial stress is above some critical level which exceeds the adhesion strength between the insulator and the conductive material a failure will occur. The availability of such experimentally derived limits for adhesion strength or warpage can underpin model-based assessments for the failure risk of 3D inkjet-printed electronics structures.

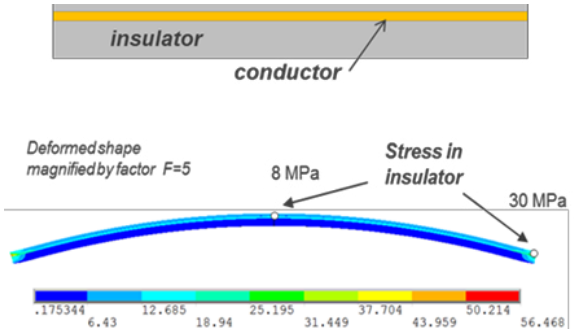


*Figure 4: Model prediction for von Mises stress and deformation of a 10-layer printed bi-material structure after release from substrate*

A main conclusion from this investigation is that unlike products in other applications printed with only one (typically polymer or metal) type material, printed electronics poses substantially increased reliability risks due to use of multiple material that come with difference in their cure shrinkage behaviour as well as in the coefficient of thermal expansion.

## 3 Condition based monitoring using data-driven models

Machine learning algorithms such as neural networks perform prognostics by taking into consideration past measured/monitored data of process performance or system operations and predicting expected future outcomes.

ISBN 978-3-8396-1001-5

### 3.1 NARX model

Nonlinear autoregressive neural network with external input (NARX) is a neural network algorithm suitable for modelling the trends of dynamic systems [10,12]. The algorithm uses past data time series of feedback and external input parameters to enable the predictions for the future outcomes of a characteristic feedback parameter. The NARX algorithm can be used either for one-step-ahead or multi-step-ahead predictions. The advantage of the NARX model is its ability to converge fast while at the same time being a general and robust data-driven model when compared to other types of neural networks.

The simplified mathematical representation of the NARX model (as a function f ) is given as:

$$y(n)= f[u(n), u(n-1),\ldots u(n-d_u), y(n-1), y(n-2),..., y(n-d_y)]$$

where y(t) is the output of the NARX network at discrete time step t, u(t) and y(t) represent the input and output of the network respectively at discrete time step t, and $d_u$ and $d_y$ are the so-called memory orders of the input and output respectively. We refer to input parameters u(t) as being external input parameters and y(t) is the feedback time series for which model predictions are made.

Figure 5 shows a conventional diagram for the NARX as it can be found in most public domain sources.

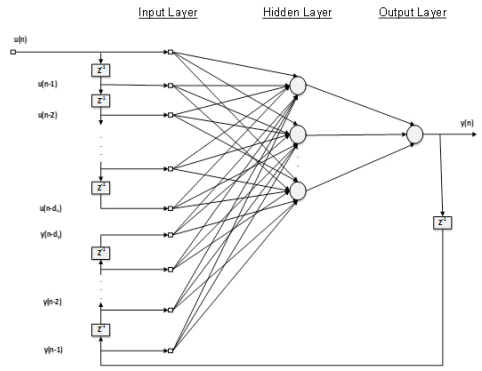


*Figure 5: NARX architecture*

The operation of the NARX algorithm is based on the fundamental principles of artificial neural networks. The model consists of a connected network of neurons which take and propagate received signals (data) from the input layer towards the output layer. Initially, past data from a feedback time series and an external time series are inserted in the input layer. Feedback time series is the term for the parameter/characteristic for which the network model is developed and prediction (forecasting) of future values are made. External time series capture data of input parameters that affect the feedback time series. Depending on the nature and level of non-linearity of the problem, the number of neurons/layers used in NARX can vary; more complex cases require the use of larger number of neurons.

### 3.2 Demonstration study

Printed conductive lines are main feature of any printed electronic device. It is very important to obtain the lowest possible resistance or to meet any user defined requirements for resistivity that might be specified.

This study case is based on data reported for the inkjet printing of meandering lines on polyethylene terephthalate substrate using a DGP 40LT-15C ink [9]. These meandering lines are printed up to 13 layers with values of resistivity varying with layer thickness during the process. Resistivity depends only on the material if no boundaries exist at distances comparable with the mean free path of the electrons in the material [9]. The work reported in [9] confirms that resistivity of silver-ink printed lines thinner than 500 nm is not constant because of significant extra scattering of electrons on the surface of the lines.

The data series of past data values for layer thickness and resistivity used to train the NARX model are detailed with figures 6. The NARX network model is realised using MATLAB software tool [10]. Stoppage criteria for the neural network is set to six validation checks with no further improvement on the validation set. As with any neural network, an existing model can be constantly updated when new data becomes available.

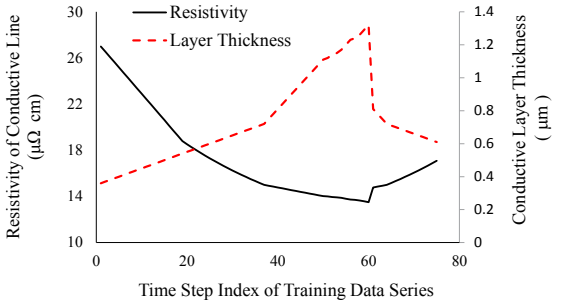


*Figure 6: Feedback (resistivity) and external input (layer thickness) data series for NARX neural network training*

The data series of the layer thickness and resistivity parameters define the input of the network at each discrete time step associated with the print of a single conductive line. At the end of printing each line measurements for line thickness and resistivity are performed. The constructed NARX model forecasts the resistivity of conductive lines that are about to be printed. In this demonstration, the NARX algorithm is set to provide five-step-ahead predictions.

The specification requirement upon which the CBM is based is that the resistivity of a conductive track should not increase above a limit of 21 μOhm.cm. In this instance, the resistivity value is used as a quality metric. Resistivity changes due to variation in the lines' sub-micrometre targeted thicknesses. In this study, the warning threshold limit is set to 20 μOhm.cm.

ISBN 978-3-8396-1001-5

The NARX model prediction results for the feedback series (resistivity monitoring) are detailed with the graph in Figure 7. Using the model, at time step 22 of the considered sequential data for 3D inkjet-printed thin film conductive lines a warning flag is raised as the forecasted five-step-ahead resistivity value is above the warning level. This information can be used to trigger a corrective process action. The prediction made is that at time step 27 the quality parameter will be above the threshold warning level of 20 µOhm.cm. Indeed, in the case of no action taken at time step 22 and assuming the printing has continued unaltered, the lines printed at step 26 and after have been characterised with resistivity values above the threshold limit.

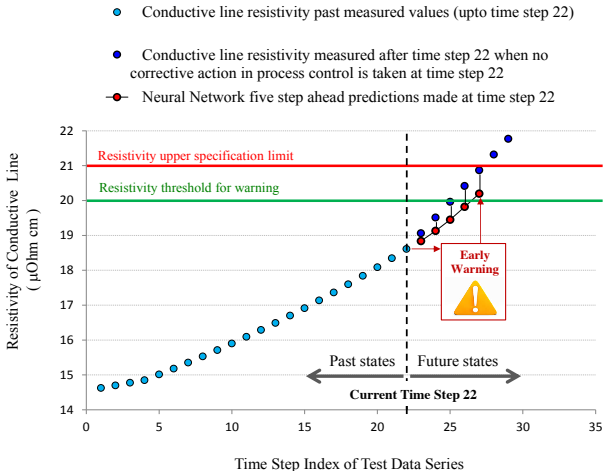


*Figure 7: NARX neural network five-step-ahead predictions for quality parameter (resistivity of conductive line) over discrete time steps*

## 4 Conclusions

The adoption of pro-active model based assessment of 3D inkjet-printed electronics products can help mitigating some common reliability and quality risks currently present with this manufacturing technology. Advanced capabilities in finite element analysis have been successfully adopted and demonstrated for the task of evaluating stresses and deformations, including product shape deviation form target geometry, in printed structures due to cure shrinkage. Cure shrinkage takes place predominantly in the out-of-plane direction. Residual stresses caused by 3D printing process have to be minimised as they can affect subsequent reliability and performance due to impact from operational and environmental loads.

Data-driven prognostics algorithms such as the NARX neural network offer online or offline capability for forecasting future outcomes of product characteristics that account for the dynamic behaviour of the printing process. This approach has been demonstrated as a diagnostics-prognostics tool that informed on electrical performance characteristics of printed conductive lines, and accurately raised a warning prior to printing out-of-specification conductive lines. Other printed electronics features related to quality, performance or reliability can be predicted or monitored with these toolsets in a similar way.

## Acknowledgements

This paper is based on work supported by the NextFactory research project funded under the European Community´s 7th Framework Programme (FP7/2007-2013) under grant agreement No. 608985

## Literature

[1] B. Berman, “3-D printing: The new industrial revolution,” Business Horizons, vol. 55, no. 2, 2012, pp. 155–162.

[2] S. M. Bidoki, D. M. Lewis, M. Clark, A. Vakorov, P. Millner and D. McGorman, “Ink-jet fabrication of electronic components,” Journal of Micromechanics and Microengineering, vol. 17, no. 5, 2007, pp. 967–974.

[3] J. Perelaer, A. W. M. de Laat, C. Hendriks and U. Schubert, “Inkjet-printed silver tracks: low temperature curing and thermal stability investigation”, Journal of Materials Chemistry, vol. 18, 2008, pp. 3209–3215

[4] ASTM F2792 Standard, "Standard Terminology for Additive Manufacturing Technologies", available at: http://www.astm.org

[5] B. Derby, “Inkjet printing ceramics: from drops to solid,” J. Eur. Ceram. Soc., vol. 31, no. 14, Nov. 2011, pp. 2543–2550

[6] J. Xiong, G. Zhang, J. Hu, and L. Wu, “Bead geometry prediction for robotic GMAW-based rapid manufacturing through a neural network and a second-order regression analysis,” J. Intell. Manuf., vol. 25, no. 1, 2012, pp. 157–163.

[7] Z. Jiang, Y. Liu, H. Chen, and Q. Hu, “Optimization of Process Parameters for Biological 3D Printing Forming Based on BP Neural Network and Genetic Algorithm,” Adv. Transdiscipl. Eng., vol. 1, 2014, pp. 351 – 358.

[8] O. Stava, J. Vanek, B. Benes, N. Carr, R. Mech, “Stress relief: improving structural strength of 3d printable objects,” ACM Transactions on Graphics, vol. 31, no. 4, 2012, Article 48.

[9] J. Salmeron et al., „Properties and Printability of Inkjet and Screen-Printed Silver Patterns for RFID Antennas“, Journal of Electronic Matreials, Vol. 43, No. 2, 2014, pp. 604-617

[10] MathWorks, Inc., MATLAB R2014a software, (http://uk.mathworks.com/)

[11] ANSYS, Inc. (www.ansys.com)

[12] J. Gomm, D. L. Yu and D. Williams, “A new model structure selection method for non-linear systems in neural modelling,” in International Conference on Computer Control (UKACC), vol. 2, no. 427, 1996, pp. 752-757